RESEARCH PAPER

RNA Biology 11:11, 1364–1374; November 2014; © 2014 Taylor & Francis Group, LLC

FMRP interacts with G-quadruplex structures in the 3′-UTR of its dendritic target Shank1 mRNA

Yang Zhang[1], Christian M Gaetano[2], Kathryn R Williams[3], Gary J Bassell[3], and Mihaela Rita Mihailescu[2,*]

[1]Graduate School of Pharmaceutical Sciences; Mylan School of Pharmacy; Duquesne University; Pittsburgh, PA USA; [2]Department of Chemistry and Biochemistry; Duquesne University; Pittsburgh, PA USA; [3]Department of Cell Biology; Emory University School of Medicine; Atlanta, GA USA

Keywords: Fragile X syndrome, G-quadruplex, Shank1 mRNA, FMRP, RGG box

Fragile X syndrome (FXS), the most common cause of inherited intellectual disability, is caused by the loss of expression of the fragile X mental retardation protein (FMRP). FMRP, which regulates the transport and translation of specific mRNAs, uses its RGG box domain to bind mRNA targets that form G-quadruplex structures. One of the FMRP *in vivo* targets, Shank1 mRNA, encodes the master scaffold proteins of the postsynaptic density (PSD) which regulate the size and shape of dendritic spines because of their capacity to interact with many different PSD components. Due to their effect on spine morphology, altered translational regulation of Shank1 transcripts may contribute to the FXS pathology. We hypothesized that the FMRP interactions with Shank1 mRNA are mediated by the recognition of the G quadruplex structure, which has not been previously demonstrated. In this study we used biophysical techniques to analyze the Shank1 mRNA 3′-UTR and its interactions with FMRP and its phosphorylated mimic FMRP S500D. We found that the Shank1 mRNA 3′-UTR adopts two very stable intramolecular G-quadruplexes which are bound specifically and with high affinity by FMRP both *in vitro* and *in vivo*. These results suggest a role of G-quadruplex RNA motif as a structural element in the common mechanism of FMRP regulation of its dendritic mRNA targets.

Introduction

Fragile X syndrome (FXS) is the most common cause of inherited intellectual disability, affecting ~1 in 4000 males and ~1 in 8000 females.[1] The syndrome is caused by an unstable expansion of a cytosine-guanine-guanine (CGG) trinucleotide repeat that silences the *fmr1* gene, resulting in the loss of expression of the fragile X mental retardation protein (FMRP).[2,3]

FMRP is produced in many tissues, being most abundantly expressed in brain and testes.[4] In neurons, FMRP is present in the cell body as well as at the synapses.[5] As a messenger RNA (mRNA) binding protein, FMRP contains two types of RNA-binding motifs: two K-homology (KH) domains and one arginine-glycine-glycine rich region (RGG) box. Additionally, it contains a nuclear localization signal (NLS) at the N-terminus and a nuclear export signal (NES) at its C-terminus, which allow it to shuttle between the nucleus and cytoplasm.[6,7] FMRP normally represses the translation of its mRNA targets, the release of this repression being coupled with its dephosphorylation in response to an activation signal, which results in a burst of local protein synthesis.[8,9] In fragile X syndrome neurons, however, a subset of dendritic proteins synthesis is constitutively elevated due to the lack of FMRP even in the absence of an activation signal.[10]

FMRP has been shown to use its RGG box domain to bind mRNA targets that form G-quadruplex structures.[11-13] A G-quadruplex is assembled from stacked G quartets that are formed by guanine residues arranged in a planar configuration by Hoogsteen-type hydrogen bonds.[14-16] G-quadruplex structures are stabilized by K^+ and Na^+ ions, with K^+ ions stabilizing better than Na^+ ions; however, at least in the case of RNA they can form even in the absence of these ions.[17,18] G-quadruplex structures have been mostly found in mRNA untranslated regions (UTR), 3′ UTR or 5′ UTR, which are known to be involved in translational regulation, particularly of growth factors, transcription factors and onco-proteins, implying that the G-quadruplex plays a role in gene expression regulation at the mRNA level.[19-21] The G-quadruplex structure located in the 3′ UTR has been proposed to act as a neurite localization signal of dendritic mRNAs, such as Shank1, PSD-95, CaMKIIa, dendrite and glycine receptor A1 subunit.[22,23]

Although it has been shown that FMRP participates in the post-transcriptional control of gene expression, the details of the exact mechanisms by which FMRP recognizes its mRNA targets and exerts its translation regulator function are not fully understood. As a translation regulator, FMRP has been reported to locally control the synthesis of proteins in dendrites, such as several components of the postsynaptic density (PSD).[24,25] PSD is a protein network attached to the postsynaptic membrane of excitatory synapses, which serves to cluster cell adhesion molecules, to recruit signaling proteins, and anchor these components to the microfilament-based cytoskeleton in dendritic spines.[26-28] For example, it has been shown that the PSD-95 expression in dendrites and controlled dendritic spine morphology are selectively and

*Corresponding author: Mihaela Rita Mihailescu; Email: mihailescum@duq.edu
Submitted: 11/08/2014; Accepted: 11/10/2014
http://dx.doi.org/10.1080/15476286.2014.996464

reversibly regulated by the FMRP phosphorylation status coupled with a microRNA miR-125a.[29]

The master scaffold proteins of the PSD, SH3 and multiple ankyrin repeat domains proteins (Shanks), regulate the size and shape of dendritic spines because of their capacity to interact with many different PSD components, such as PSD-95 and F-actin.[26,30] The Shank family of genes, composed of *Shank1*, *Shank2* and *Shank3*, has been linked to autism spectrum disorders, upon the findings of sequence changes in these genes, which include missense, frame shift, splice site mutations, microdeletions and point mutations.[31] The shank proteins interact with all major types of glutamate receptors and with other scaffolding and signaling proteins, however, the mechanisms by which such interactions are regulated are not known.[31] The localization of mRNA transcripts for Shank1 and Shank3 is on dendrites, which makes Shanks have significant effects on spine morphogenesis and development of spines on non-spiny neurons.[32,33] Due to their effect on spine morphology, altered translational regulation of Shank1 transcripts may contribute to the FXS pathology.[34] Increased Shank1 levels have been found in PSD fractions obtained from FMRP-deficient mice.[35] It has also been shown that Shank1 mRNA is an *in vivo* FMRP target,[36] which is supported by further molecular evidence that FMRP represses the translation of Shank1 mRNA via interactions with its 3′ UTR.[35] Given that a G-quadruplex structure is predicted to exist in Shank1 mRNA 3′ UTR, we hypothesized that the regulation of Shank1 translation is dependent on the FMRP recognition of these G-quadruplex-forming sites in its 3′ UTR.[22]

To test this hypothesis, in this study, we first used biophysical methods to characterize the 3′ UTR of human Shank1 RNA, showing directly the existence of two sequential G-quadruplex structures. We have also determined that both FMRP and its phosphorylated mimic bind with high affinity to these G-quadruplexes within the Shank1 3′-UTR, *in vitro*. These results were also validated *in vivo* by the findings that each of the Shank1 G-quadruplex structures is sufficient for interactions with FMRP in mouse brain lysates. The results of this study suggest that FMRP might employ a common mechanism to recognize dendritic mRNAs components of PSD by interacting directly with the G-quadruplex structures present in their 3′-UTR.

Results

Two G-quadruplex structures are present in the 3′ UTR of Shank1 RNA

We hypothesize that the G-quadruplex structure mediates the interactions of FMRP with Shank1 mRNA 3′ UTR. Thus, we used the quadruplex forming G-Rich sequences (QGRS) mapper, a web-based server for predicting G-quadruplexes in nucleotide sequences, to identify G-rich sequences in the human Shank1 3′ UTR RNA that have the potential to form G-quadruplex structures (http://bioinformatics.ramapo.edu/QGRS/index.php). Two G rich sequences adjacent to each other in the 3′ UTR were identified, which were named Shank1a RNA and Shank1b RNA in this study (**Table 1**). The Shank1a and Shank1b mRNA sequences were *in vitro* transcribed and ^{1}H NMR spectroscopy experiments were performed to examine the existence of G-quadruplex structures in their fold, by monitoring the imino proton resonance region. Resonances in the region 10–12 ppm report on guanine imino protons involved in the formation of G-quadruplex structures, whereas those located between 12–14.5 ppm report upon guanine and uracil imino protons involved in Watson-Crick basepairs.[37] Spectra were acquired for both Shank1a and Shank1b RNA samples in the presence of increasing concentrations of KCl, and, as seen in **Fig. 1**, even in the absence of K^+ ions, for both sequences there are broad resonances centered around 11 ppm, signature of the G-quadruplex structure. As KCl is titrated in the samples, in the case of Shank1a sharper resonances become apparent on the broad envelope centered around 11 ppm, indicating the G-quadruplex structure stabilization (**Fig. 1A**). Minimal changes are observed in the imino proton resonance of Shank1b RNA in the presence of K^+ ions (**Fig. 1B**). No resonances are observed in the region 12–14.5 ppm, indicating that Shank1a and Shank1b mRNAs do not form alternate structures involving Watson-Crick base pairs. Taken together the ^{1}H NMR spectroscopy results indicate that both G-rich RNA sequences in Shank1 RNA form G-quadruplex structures even in the absence of KCl, the G-quadruplex structure formed by the Shank1a being further stabilized by the presence of K^+ ions.

The conformations of the G-quadruplex structures formed by Shank1a and Shank1b RNA were analyzed by 15% native gel electrophoresis in the presence of increasing KCl concentrations in the range 0–50 mM (**Fig. 2A and B**). Two bands are present in Shank1a RNA in the absence of KCl (**Fig. 2A**, lane 1), indicating the co-existence of alternate conformations. Upon increasing the KCl concentration the equilibrium between the two conformations shifts, as reflected by the decrease in the intensity of the lower migrating band (**Fig. 2A**, compare lanes 1-5). Similarly, two bands are present in the native gel of Shank1b RNA in the absence of KCl (**Fig. 2B**, lane 1), which collapse into a broad band upon the addition of K^+ ions (**Fig. 2B**, lanes 2-5), indicating the co-existence of alternate conformations in Shank1b RNA. These results are consistent with the ^{1}H NMR spectroscopy data, as the G-quadruplex imino protons gave rise to resonances on a broad envelope indicative of a dynamic exchange between conformations.

To obtain further information about the fold of the G-quadruplex structures present in Shank1 RNA 3′ UTR, CD spectroscopy experiments were performed in the presence of different concentrations of KCl (**Fig. 2C and D**). In the absence of KCl, a negative band was observed at 240 nm and a positive one at 265 nm, for both Shank1a and Shank1b RNA sequences, the typical CD signature of parallel G-quadruplexes (**Fig. 2C and 2D**, 0 mM KCl).[38,39] Once the KCl concentration was increased to 10 mM (**Fig. 2C**), the intensities of both the positive and negative bands increased significantly for Shank1a RNA, indicating that KCl facilitates the stabilization of its G-quadruplex structure. In contrast, in the case of Shank1b RNA (**Fig. 2D**), the intensities of the bands at 260 nm and 240 nm did not increase significantly, indicating that the G-quadruplex formed by this

Table 1. Sequences of the Shank1a and Shank1b fragments used in this study. The numbers refer to the GenBank accession number AY461451.1. The guanines proposed to be implicated in G-quadruplex formation are underlined. The adenines replaced by 2AP to produce the fluorescently labeled Shank1a_18AP and Shank1b_242AP are bolded.

Shank1a (nt 423-450) 18	
	5′ GGGGUUGGGGAGGGUGUA**A**GGGGGUGGGG 3′
Shank1b (nt 452-481) 24	
	5′ GGGGAGGAGAGGUCGGGGUGGGG**A**GUGGGG 3′

sequence is stable even in the absence of the K^+ ions. The further increase of the KCl concentration at 25, 50 and 150 mM (**Fig. 2C and D**) did not result in a significant further increase of the intensities of these bands for either Shank1a and Shank1b, suggesting that 10 mM KCl is sufficient to stabilize the G-quadruplex structure of Shank1a RNA, similarly to the ^{1}H NMR spectroscopy results. Taken together, the previous results and the CD spectroscopy experiments indicate that Shank1a RNA forms two alternate parallel G-quadruplex structures, one of which is further stabilized by the presence of K^+ ions. Shank1b RNA forms alternate G-quadruplex structures that are stable even in the absence of K^+ ions.

To determine if the G-quadruplex structures formed by Shank1 RNA are intermolecular or intramolecular, UV spectroscopy thermal denaturation experiments were employed. For intermolecular G-quadruplexes, the melting temperature, T_m, depends on the RNA concentration, C_T:[40]

$$\frac{1}{Tm} = \frac{R(n-1)}{\Delta H^{\circ}_{vH}} lnC_T + \frac{\Delta S^{\circ}vH - (n-1)R\ln 2 + R\ln n}{\Delta H^{\circ}_{vH}} \quad (1)$$

where n is the number of strands, R is the gas constant and ΔH^0_{vH} and ΔS^0_{vH} are the Van't Hoff thermodynamic parameters. For intramolecular conformations, n equals to 1. The melting temperature T_m is therefore independent of the total RNA concentration C_T.

$$n = 1 \text{ and } \frac{1}{Tm} = \frac{\Delta S^{\circ}vH}{\Delta H^{\circ}vH} \quad (2)$$

Several Shank1 RNA concentrations in the range 5–25 μM in 10 mM cacodylic acid, pH 6.5, were thermally denatured at a heating rate of 0.2°C/min and the absorbance changes were monitored at 295 nm, wavelength shown to be most sensitive to G-quadruplex dissociation.[41] At all RNA concentrations investigated, a single hypochromic transition is present in the UV thermal denaturation profile of Shank1a and Shank1b RNAs, typical of G-quadruplex structure unfolding (**Fig. 3A and B**). The UV thermal denaturation profile of Shank1a RNA in 2.5 mM KCl contains a hypochromic transition with a T_m ~73°C (**Fig. 3A**), which is attributed to its G-quadruplex structure dissociation.[38] A hypochromic transition with a T_m ~76°C was observed in Shank1b RNA UV thermal denaturation profile in the presence of 10 mM KCl (**Fig. 3B**). The melting temperatures of each hypochromic transition at different RNA concentrations were plotted against the RNA concentration and for both, Shank1a and Shank1b G-quadruplexes, the melting temperature is independent of the RNA concentration (**Fig. 3C and D**), indicating that these G-quadruplex structures are intramolecular. In the presence of 10 mM KCl, the Shank1b RNA G-quadruplex melting temperature is 76°C (**Fig. 3D**) versus a very similar T_m (73°C) of the Shank1a RNA G-quadruplex at only 2.5 mM KCl (**Fig. 3C**), indicating that Shank1a RNA forms a more stable intramolecular G-quadruplex structure than Shank1b RNA. After establishing the intramolecular conformation of Shank1 G-quadruplexes, the UV hypochromic transition was fitted with an independent two-state model (equation 3, materials and methods) (**Fig. 3E, F**). The calculated melting temperatures based on the obtained thermodynamic parameters are 72.7 ± 0.9°C for Shank1a G-quadruplex at 2.5 mM KCl and 75.8 ± 0.8°C Shank1b G-quadruplex in the presence of 10 mM KCl. The

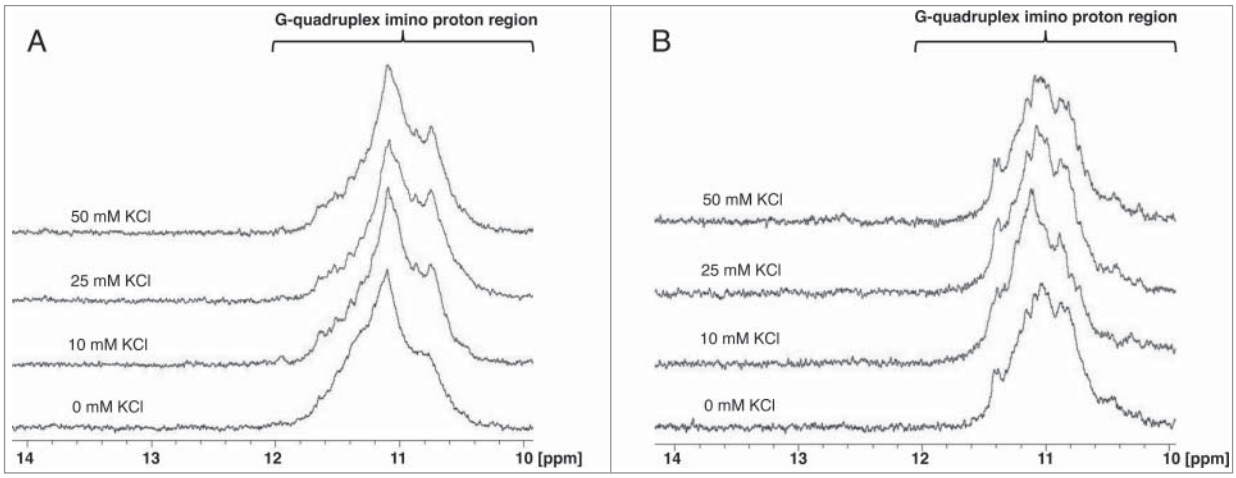

Figure 1. ^{1}H NMR spectra of the imino proton region of Shank1a **(A)** and Shank1b **(B)** RNA in the presence of increasing concentrations of KCl in the range 0–50 mM.

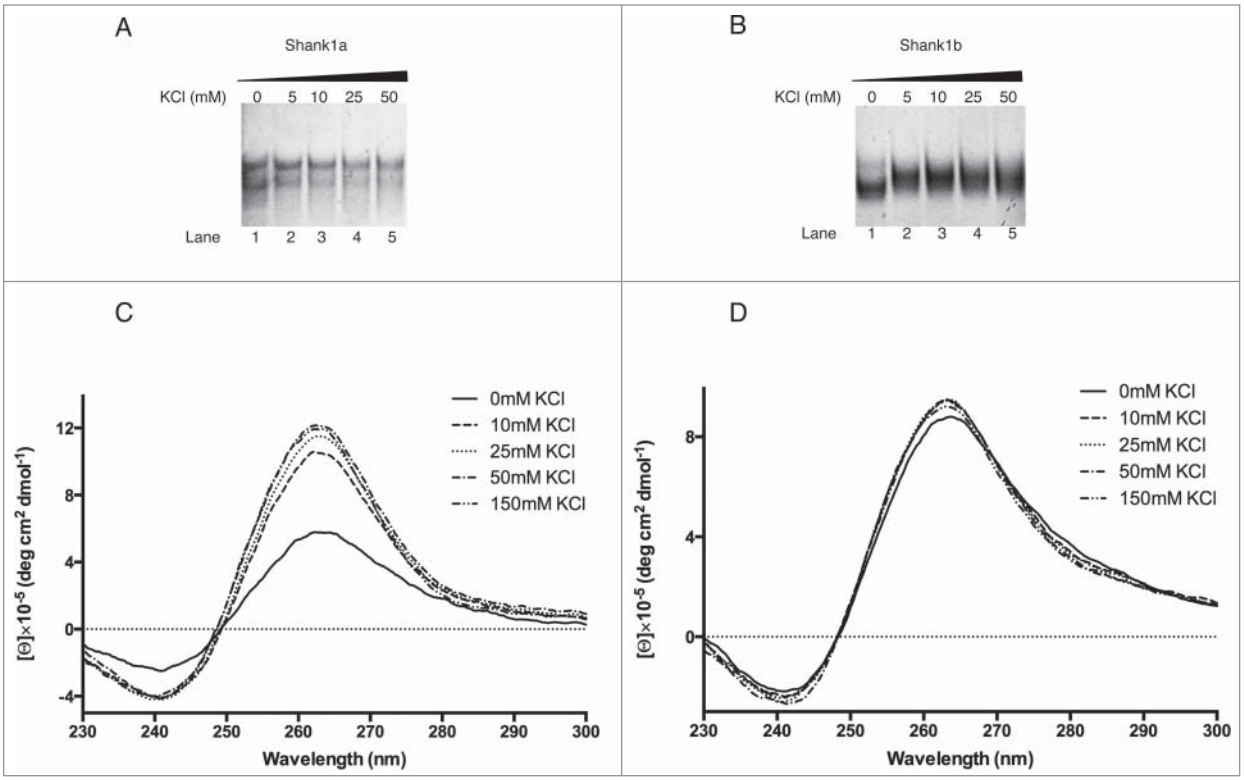

Figure 2. Native polyacrylamide gel electrophoresis (PAGE) of 15 μM Shank1a **(A)** and Shank1b **(B)** RNAs at various KCl concentrations: 0 mM (lane 1), 5 mM (lane 2), 10 mM (lane 3), 25 mM (lane 4) and 50 mM (lane 5). The CD spectra of 10 μM Shank1a **(C)** and Shank1b **(D)** RNAs prepared in 10 mM cacodylic acid at various KCl concentrations showing the presence of a parallel G-quadruplex structures stabilized by KCl.

biophysical and biochemical analysis of Shank1 RNA has shown that both selected sequences adopt very stable parallel G-quadruplex structures that form in an intramolecular manner. Additionally, there is equilibrium between alternate G-quadruplex conformations existing in the Shank1a and Shank1b RNAs respectively and the stability of Shank1a G-quadruplex is further enhanced by the presence of K^+ ions.

Shank1a and Shank1b G-quadruplex RNA interactions with FMRP

Next, we employed fluorescence spectroscopy to determine if FMRP interacts with the G-quadruplexes formed by Shank1a and Shank1b RNAs. Two fluorescently labeled RNAs (named Shank1a_18AP and Shank1b_24AP) were constructed by replacing the adenine at position 18 in Shank1a and at position 24 in Shank1b with its fluorescent analog 2-aminopurine (2AP) (circled in **Fig. 4**, and bolded in **Table 1**). The steady-state fluorescence of 2AP is very sensitive to its surrounding environment, especially to stacking interactions. At its excited state, the fluorescent properties of the 2AP are strongly dependent on the electron transfer quenching process from guanine.[42] The 2AP fluorophore is predicted to be part of the long loop in the Shank1a and of the shorter one in the Shank1b G-quadruplex structures (**Fig. 4**), its steady-state fluorescence being expected to change upon FMRP binding. Initially we analyzed the binding of the FMRP RGG box domain, which has been shown to recognize specifically G-quadruplex mRNA.[12,13,43,44] As predicted, a decrease in the steady-state fluorescence intensity was observed for both Shank1a_18AP and Shank1b_24AP upon the FMRP RGG box titration (**Fig. 4C, D**), and the binding curves were fitted with equation 4 (materials and methods) to obtain the dissociation constant of each of the Shank1 RNA: FMRP RGG box complexes. The binding experiments were performed in triplicate, each binding curve being fitted independently, and the dissociation constant values were calculated as the average of the Kd values obtained from each experiment. A dissociation constant of 68 ± 4 nM was determined for the Shank1a_18AP RNA: FMRP RGG box complex, and of 151 ± 32 nM for the Shank1b_24AP RNA: FMRP RGG complex (**Fig. 4C and D**), indicating that Shank1a RNA has higher binding affinity than Shank1b RNA. Electromobility gel shift assays of the Shank1a and Shank1b RNA complexes with the FMRP RGG box are supporting this conclusion as well (Supplementary **Fig. S1**). The Kd values measured for Shank1a_18AP and Shank1b_24AP RNA: FMRP RGG box complexes are larger than the dissociation constants reported previously for the FMRP RGG box binding to other G-quadruplex forming mRNA targets, which ranged between 1-20 nM.[13,43,45,46] This could be due to the fact that both Shank1a and Shank1b G-quadruplexes are predicted to consist of four G quartet planes surrounded by an extended longer loop of 8∼10 nucleotides and a short one of 2∼3 nucleotides (**Fig. 4A and B**), whereas the previous G-quadruplexes

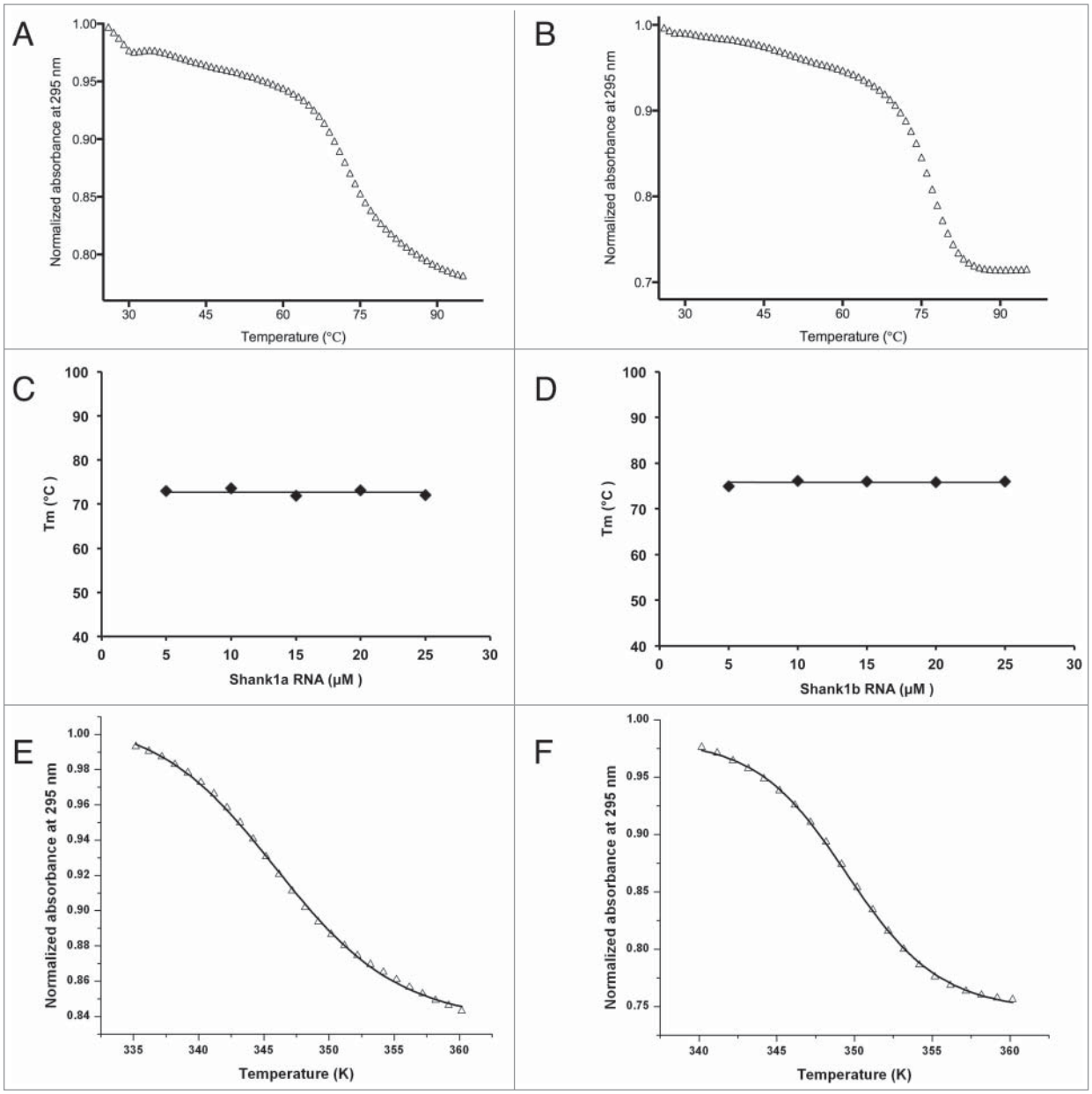

Figure 3. The UV thermal denaturation profiles of Shank1a RNA at 2.5 mM KCl **(A)** and Shank1b RNA at 10 mM KCl **(B)** in the presence of 10 mM cacodylic acid, pH 6.5. The melting temperatures of Shank1a **(C)** and Shank1b **(D)** G-quadruplexes were plotted versus the RNA concentrations showing that the melting temperature is independent of the RNA concentration. The UV hypochromic transitions of Shank1a RNA at 2.5 mM KCl **(E)** and Shank1b RNA at 10 mM KCl **(F)** were fitted equation 3 (materials and methods) that assumes a two state model.

investigated are formed by two-plane G-quartet surrounded by shorter loops containing between 1-3 nucleotides.

Once we established that both Shank1a and Shank1b G-quadruplexes are bound with high affinity and specificity by the FMRP RGG box we analyzed their interactions with the full-length FMRP. It has been shown that FMRP regulates the transport and translation of multiple messenger RNA targets involved in neuronal development.[46-48] The mechanism of how FMRP exerts its translation regulator function is still under investigation, however, previous findings have suggested that phosphorylation plays a role in the FMRP translation regulation function.[8,29,50] Aiming to understand if the FMRP phosphorylation results in any potential binding affinity difference to the G-quadruplex forming Shank1 RNA, we employed the previously created phosphorylated mimic form of FMRP isoform 1, FMRP S500D, in which serine 500 was mutated to aspartic acid.[29,50,51] The FMRP ISO1 and FMRP S500D were recombinantly expressed in *E. coli* cells.

Once again we used the fluorescently labeled Shank1a_18AP and Shank1b_24AP G-quadruplexes, monitoring the steady-state fluorescence changes in the emission of the 2AP reporter while titrating either FMRP ISO1 or FMRP S500D. The experiments

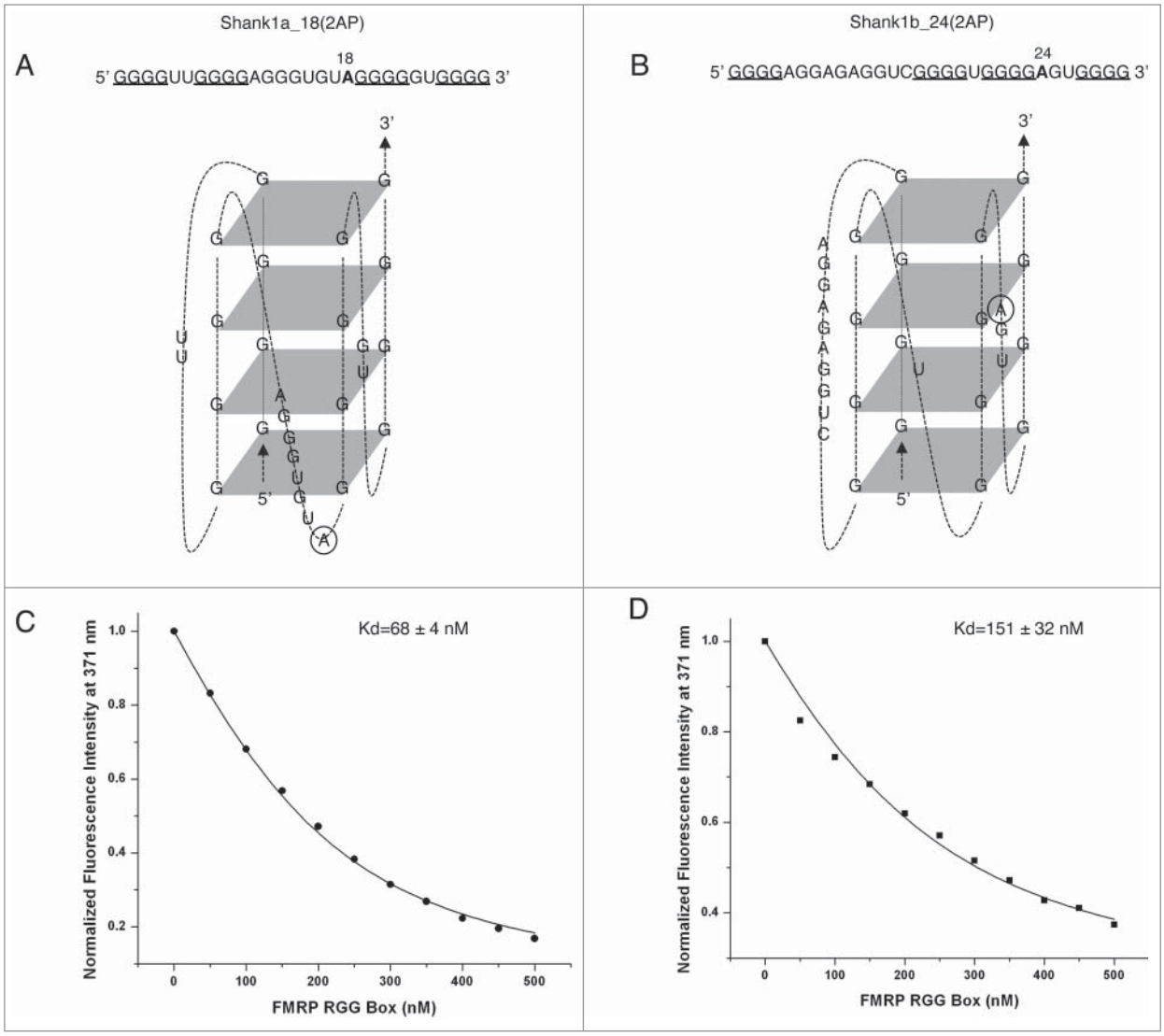

Figure 4. Proposed G-quadruplex structures adopted by Shank1a **(A)** and Shank1b RNA **(B).** The fluorescently labeled Shank1a_18AP and Shank1b_24AP RNAs were constructed by replacing the adenine at position 18 and position 24, respectively. The FMRP RGG box was titrated into 200 nM of the fluorescently labeled Shank1a_18AP **(C)** and Shank1b_24AP **(D)** in the presence of 1 μM HCV peptide. The steady-state fluorescence data was fitted with equation 4 (materials and methods). The reported Kd values represent the average of three Kd values in the triplicates.

were performed in triplicate and the binding curves were fitted with equation 4 (materials and methods) to determine the dissociation constants of the Shank1 RNA: FMRP complexes (**Fig. 5**). The dissociation constant of Shank1a_18AP RNA: FMRP ISO1 complex, was determined to be Kd = 198 ± 28 nM (**Fig. 5A**), whereas that of the Shank1b_24AP RNA: FMRP ISO1 complex was Kd = 384 ± 66 nM, respectively (**Fig. 5C**). For both RNAs, these values are significantly higher than the respective Kds measured for their complexes with the RGG box, likely due to a more complex structure of the full-length protein and therefore possible reduced accessibility of the RGG box. The reduced binding affinity from the FMRP RGG box to the full-length FMRP isoform was also observed for the other FMRP G-quadruplex forming RNA targets, such as Semaphorin 3F mRNA (Kd = 0.7 ± 0.3 nM for binding to the FMRP RGG box versus Kd = 104 ± 11 nM for the FMRP ISO1).[13,52] However, the trend observed in the case of the Shank1 RNA: FMRP RGG box complexes is maintained, namely, FMRP ISO1 has higher affinity for Shank1a than for Shank1b G-quadruplex. Nonetheless, it is worthwhile to mention that the dissociation constants of the complexes formed by each RNA with FMRP ISO1 translates into a free energy of binding of $\Delta G^0_b = -9.1 \pm 0.1$ kcal/mol for Shank1a_18AP and of $\Delta G^0_b = -8.7 \pm 0.2$ kcal/mol for Shank1b_24AP respectively, resulting in a difference in binding free energy of only 0.4 kcal/mol (**Table 2**).

Similarly, the dissociation constant of the Shank1a_18AP: FMRP S500D complex was determined to be Kd = 281 ± 28 nM (**Fig. 5B**), whereas that of the Shank1b_24AP: FMRP S500D complex was Kd = 214 ± 22 nM (**Fig. 5D**). The

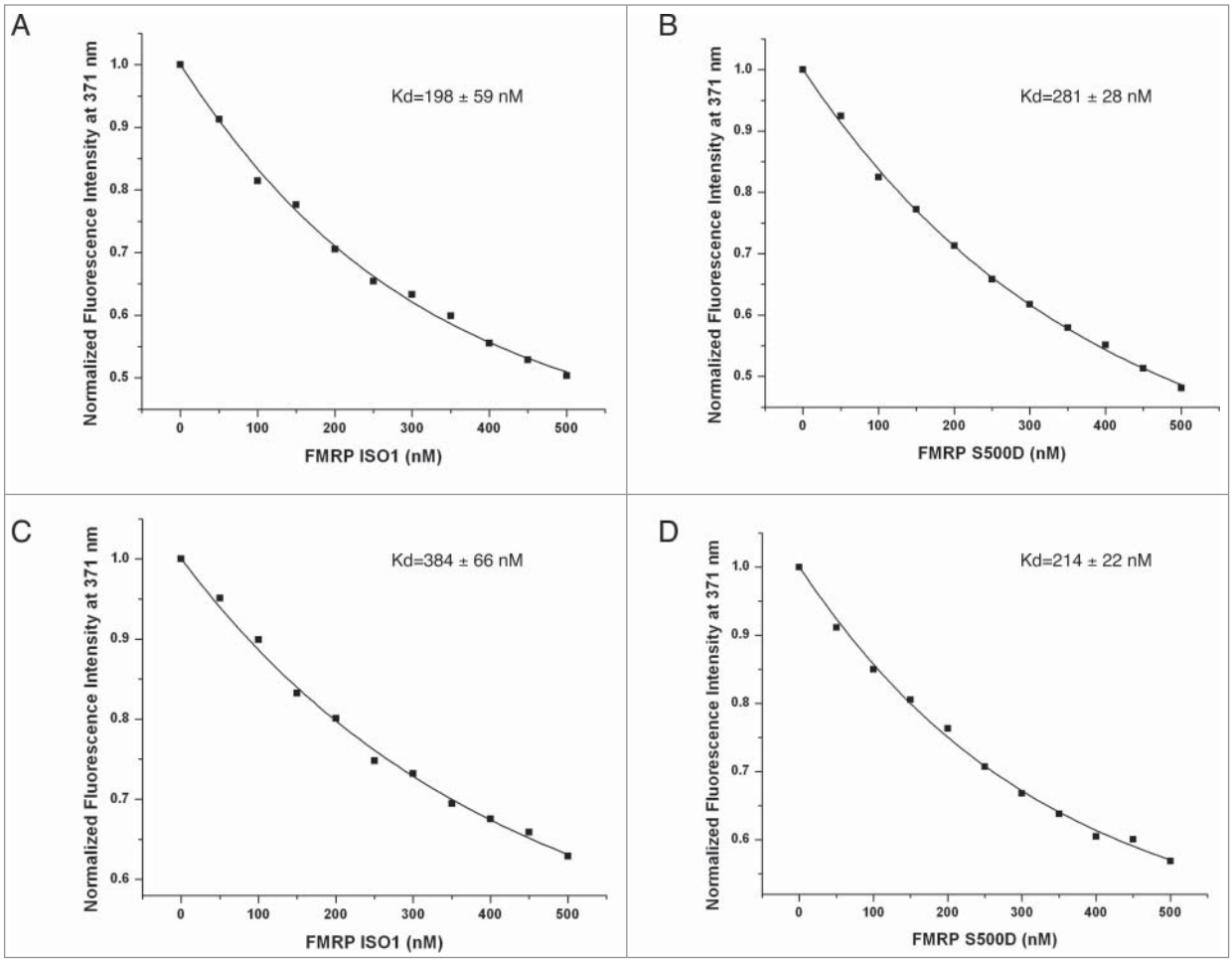

Figure 5. The FMRP ISO1 and FMRP S500D were titrated into 200 nM of the fluorescently label Shank1a_18AP **(A, B)** and Shank1b_24AP **(C, D)** RNAs in the presence of 1 μM BSA. The reported Kd value represents the average of three Kd values in the triplicates.

analysis of these Kd values suggests an opposite trend from FMRP ISO1, namely FMRP S500D binds tighter to Shank1b than to Shank1a G-quadruplex. However, the binding free energies for the Shank1a_18AP: FMRP S500D ($\Delta G^0_b = -8.9 \pm 0.1$ kcal/mol) and Shank1b_24AP: FMRP S500D ($\Delta G^0_b = -9.1 \pm 0.1$ kcal/mol) complexes calculated based on these dissociation constants do not differ from each other within the experimental error (**Table 2**).

The binding free energies of FMRP ISO1 and FMRP S500D for Shank1a_18AP are also not different from each other within experimental error (**Table 2**), a similar trend being observed for the binding free energies of FMRP ISO1 and FMRP S500D to Shank1b_24AP. These results indicate that the posttranslational modification of phosphorylation does not modulate the translation regulator function of FMRP through different binding affinity to its G-quadruplex forming targets. The trend was also observed on a FMRP binding sequence (FBS), located in FMRP's own mRNA, which was bound with similar affinity by FMRP ISO1 and FMRP S500D.[53] Additionally, this conclusion is supported by a recent study showing that equal amounts of wild-type GST-FMRP and GST-FMRP S500D were pulled down by a G-quadruplex containing PSD-95 RNA fragment or a U-rich HOXB8 RNA fragment, two other FMRP mRNA targets.[54]

Table 2. Dissociation constants and binding free energy of Shank1 RNA binding with the FMRP ISO1 and FMRP S500D.

Complexes	Dissociation constant (Kd)	Binding free energy (ΔG^0_b)
Shank1a: ISO1	198 ± 59 nM	−9.1 ± 0.1 kcal/mol
Shank1b: ISO1	384 ± 66 nM	−8.7 ± 0.2 kcal/mol
Shank1a: S500D	281 ± 28 nM	−8.9 ± 0.1 kcal/mol
Shank1b: S500D	214 ± 22 nM	−9.1 ± 0.1 kcal/mol

Finally, we confirmed that the interactions between the Shank1 mRNA 3′ UTR and endogenous FMRP from brain tissue are mediated by the recognition of the G-quadruplex structures of Shank1a and Shank1b, by performing a biotin-RNA pull down assay using the biotin labeled Shank1a and Shank1b probes that were incubated with lysates from E17 mouse brain and then precipitated with NeurAvidin agarose. Western blot analysis revealed an association of FMRP, but not SMN, with Shank1 probes (**Fig. 6**).

Discussion

Aiming to investigate if there is a common mechanism by which FMRP recognizes its dendritic mRNA targets, and based on the previous findings that 3′ UTR of Shank1 RNA is an *in vivo* target of FMRP, we hypothesized that its interaction with Shank1 mRNA is dependent on the recognition of the RNA G-quadruplex structure.[35]

Our results revealed the existence of two G-quadruplex structures, Shank1a and Shank1b RNAs, located adjacent to each other in the Shank1 3′ UTR. Both G-quadruplexes formed by Shank1a and Shank1b fragments have a parallel fold and are intramolecular. Next we examined the interactions of Shank1a and Shank1b RNA G-quadruplexes with the isolated FMRP RGG box, as well as with the full length FMRP ISO1 and its phosphorylated mimic FMRP S500D. Our results show that the FMRP RGG box has a higher binding affinity to both Shank1a and Shank1b, as compared with the affinity of the full length FMRP ISO1 and FMRP S500D, possibly due to the structural complexity of the full-length protein and therefore the reduced accessibility of the RGG box. FMRP ISO1 binds with higher affinity to the Shank1a G-quadruplex, result confirmed also by FMRP pull-down assays from E17 mouse brain lysates.

Taken together, our results provide direct biophysical evidence that the G-quadruplex RNA motif exists in a neurite targeted mRNAs, which was implied by other indirect methods,[22] but more importantly, document that the interactions of FMRP with Shank1 mRNA are mediated by the recognition of G-quadruplex structures formed within the 3′ UTR of Shank1 RNA. The present study has important implications to suggest a specific molecular mechanism that may be impaired in fragile x syndrome, and result in dysregulated mRNA localization or local protein synthesis in dendrites and at synapses.

To further reveal the biological function of this RNA motif found in the human 3′ UTR of Shank1 mRNA, we searched the Shank1a and Shank1b G-quadruplex forming sequences in GeneBank database. Interestingly, one of the selected sequences that adopts a more stable G-quadruplex structure recognized by FMRP with a higher binding affinity, Shank1a RNA, exists also in the Shank1 mRNA of *Rattus norvegicus*, *Mustela putorius furo* and *Macaca fascicularis*, indicating its conservation in mammals. Shank1b RNA is conserved only in *Macaca fascicularis* ′ Shank1 mRNA. Accordingly, we reason that the higher conservation of Shank1a mRNA in mammals may indicate its functional importance in mediating the interactions with FMRP to regulate dendritic mRNA expression.

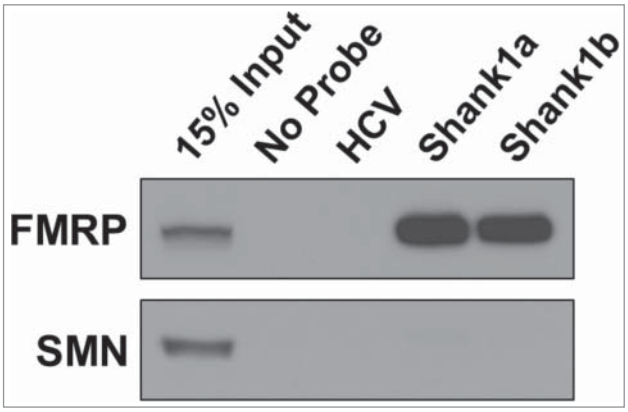

Figure 6. FMRP recognizes the Shank1 G-quadruplex structures *in vivo*. 5′ biotin-labeled Shank1a, Shank1b and HCV RNA probes were incubated with E17 mouse brain lysate. Probes were precipitated with Neutravidin agarose beads and co-purified FMRP and SMN protein was assessed by immunoblot.

Previous findings have shown that nonphosphorylated FMRP is associated with actively translating polyribosomes, while the phosphorylated form interacts with stalled ribosomes, suggesting a role of phosphorylation in modulating the translation regulation function of FMRP.[50] Accordingly, one assumption might be that the phosphorylated form of FMRP represses the gene translation by negatively influencing its binding affinity to its mRNA targets. However, we found that the binding free energies of FMRP ISO1 and FMRP S500D do not differ significantly for either Shank1a or Shank1b G-quadruplexes, suggesting that the FMRP phosphorylation would not mediate its translation regulatory function by affecting its interactions with G-quadruplex mRNA. A recent study is in agreement with our results, suggesting that the FMRP phosphorylation affects its interactions with Ago2, a protein component of the RNA interference silencing complex (RISC) in the miRNA pathway.[29]

FMRP has been linked to the miRNA pathway.[29,55] It has been shown that miR-125b, miR-132 and miR-125a, as well as several other miRNAs, are associated with FMRP in mouse brain.[29,55] One of the miRNA targets, NMDA receptor subunit NR2A, is negatively regulated through its 3′ UTR by FMRP collaborating with miR-125b in hippocampal neurons.[55] Similarly, the expression of PSD-95 is bi-directionally controlled by miR-125a and the phosphorylation status of FMRP.[29] FMRP phosphorylation status was shown to regulate interactions between FMRP and RISC/miR-125a rather than FMRP interaction with mRNA[29], which is also consistent with our results here. Considering the role of the miRNA pathway in FMRP functioning as a translation regulator, it is possible that FMRP may also regulate the translation of its target Shank1 mRNA via miRNA involvement. We have identified miRNAs associated with FMRP in mouse brain that are also complementing with these two G-quadruplex forming sequences in 3′ UTR of Shank1 mRNA. It will be necessary to further investigate the interactions among FMRP, Shank1 mRNA and miRNAs to analyze if miRNAs play a role in FMRP regulating Shank1 mRNA translation mediated by G-quadruplex RNA motif. This study serves as the molecular groundwork to determine if the FMRP regulation of dendritic mRNA translation and synaptic protein synthesis is modulated by G-quadruplex mRNA recognition in conjunction with the miRNA pathway. Our results grant the search for such a link between the microRNA pathway, FMRP and Shank1 mRNA, which will contribute to our understanding of how the absence of FMRP disrupts this regulatory process in FXS.

Materials and Methods

RNA oligonucleotides

Quadruplex forming G-Rich Sequences (QGRS) mapper (http://bioinformatics.ramapo.edu/QGRS/index.php), a web-based server for predicting G-quadruplexes in nucleotide sequences, was used to identify G-rich sequences in the human Shank1 3′ UTR RNA (GeneBank accession number AY461451.1). The sequences with highest G score, which indicates a high potential to form G-quadruplex structures, named Shank1a RNA and Shank1b RNA in this study were synthesized using the designed synthetic DNA templates (TriLink BioTechnologies, Inc.) by T7 RNA polymerase driven *in vitro* transcription reactions (**Table 1**). The RNA oligonucleotides were purified by 20% 8 M urea denaturing polyacrylamide gel electrophoresis and electrophoretic elution, followed by extensive dialysis against 10 mM cacodylic acid, pH 6.5.

The fluorescencently labeled single stranded oligonucleotides, chemically synthesized by Dharmacon, Inc., were constructed by replacing the adenine at position 18 and 24 in the original RNA sequences with its fluorescent analog 2-aminopurine (2AP) to give Shank1a_182AP and Shank1b_24AP, respectively (**Table 1**). Biotinylated Shank1a and Shank1b RNA probes were chemically synthesized by Dharmacon, Inc.

Unless otherwise specified, all RNA oligonucleotides were annealed by heating in boiling water at 95°C, followed by slow cooling at room temperature.

Peptides synthesis

The FMRP RGG box (amino acids 527-558) and the HCV core peptide (combined sequences of amino acids 2-23 and 38-74) were chemically synthesized and purified by the Peptide Synthesis Unit at the University of Pittsburgh, Center for Biotechnology & Bioengineering.

Expression and purification of recombinant FMRP ISO1 and FMRP S500D

The pET-21a-FMRP plasmid, encoding ISO1 fused with a C-terminal 6x histidine tag, was a gift from Dr. Bernhard Laggerbauer.[56] A phosphorylated mimic of the FMRP ISO1, FMRP S500D, was designed by replacing serine 500 with aspartic acid to mimic phosphorylation.[50] The pET-21a-FMRP FMRP S500D plasmid was produced by GenScript USA, Inc. The FMRP ISO1 and FMRP S500D were recombinantly expressed, purified and dialyzed as described.[56, 57] Briefly, each plasmid was transformed into the Rosetta 2(DE3) pLysS *E. coli* cell line, cells were incubated at 37°C, 250 rpm until an OD_{600} of 0.8–1.0, and target protein expression was induced by adding FMRP S500Dropyl β-D-1-thiogalactopyranoside to 1 mM, and incubating the cells at 25°C, 250 rpm for 12 h. Cells were harvested and lysed, and each FMRP isoform was purified using Ni-NTA Superflow resin (Qiagen).[57] Purified proteins were concentrated using dialysis tubing filled with polyethylene glycol (PEG) 20,000.[58] The two isoforms were dialyzed into a buffer devoid of K^+ and Na^+, suitable for the analysis of their binding activity to G-quadruplex forming mRNAs. Dialysis was performed in the presence of 5% glycerol and 1 mM EDTA with the gradual removal of imidazole.[55]The concentration of the FMRP isoforms was determined by A_{280} using the same molar extinction coefficient of 46,370 $M^{-1}cm^{-1}$ for ISO and FMRP S500D.[59,60] Successful production of FMRP isoform was analyzed using 10% tris-glycine sodium dodecyl sulfate-polyacrylamide gel electrophoresis (SDS-PAGE) and visualized using Coomassie blue.

UV spectroscopy thermal denaturation

UV thermal denaturation curves were acquired using a Varian Cary 3E UV-Visible Spectrophotometer with a Peltier temperature control cell holder. Samples were annealed prior to performing the experiments in the presence of various concentrations of KCl in 10 mM cacodylic acid, pH 6.5. Samples and reference cells were covered with 200 μL of mineral oil to prevent evaporation at high temperature. The RNA samples were heated from 25 to 95°C at a rate of 0.2°C/min, and absorbance points were recorded at every 1°C at 295 nm, wavelength identified to be most sensitive to G-quadruplex dissociation.[41]

The hypochromic transition of the G-quadruplex dissociation in Shank1a RNA and Shank1b RNA was identified and fitted with an assumed independent two state model:

$$A(T) = \frac{A_U + A_F e^{\frac{-\Delta H^\circ}{RT}} e^{\frac{\Delta S^\circ}{R}}}{e^{\frac{-\Delta H^\circ}{RT}} e^{\frac{\Delta S^\circ}{R}} + 1} \quad (3)$$

where A_U and A_F respectively represent the absorbance of the unfolded and native G-quadruplex structures, and R is the gas constant.

Circular dichroism (CD) spectroscopy

The CD spectra were recorded on a Jasco J-810 spectropolarimeter at 25°C. The G-quadruplexes formation in 10 mM cacodylic acid, pH 6.5, was monitored as increasing amounts of KCl were titrated from a 2 M stock solution to a final concentration of 150 mM. The spectra were measured between 200 and 350 nm and corrected for solvent contributions and dilutions. Each spectrum was scanned seven times with 1 s response time and a 2 nm bandwidth. For the binding studies, increasing amounts of the FMRP RGG peptide (0–80 μM) were titrated into a fixed concentration of RNA (10 μM) in 10 mM cacodylic acid, pH 6.5, and 25 mM KCl.

^{1}H NMR spectroscopy

The one dimensional ^{1}H NMR spectra of the RNA oligonucleotides were acquired at 25°C on a 500 MHz Bruker AVANCE spectrometer. Water suppression was carried out by using the Watergate pulse sequence.[61] Maximum concentrations of RNA samples (~200 μM) were prepared in 10 mM cacodylic acid buffer, pH 6.5, in a 90% H_2O/10% D_2O ratio. G-quadruplex formation was observed by titrating increasing concentrations of KCl from a 2 M stock to each sample and monitoring the imino proton resonance region.

Native polyacrylamide gel electrophoresis (PAGE)

10 μM of RNA samples in the presence of various concentrations of KCl were annealed by boiling for 5 minutes followed by cooling down at room temperature for 10 minutes, prior to their use in native gel electrophoresis. The 20% native gels in 0.5X Tris/Borate/EDTA buffer were run at 4°C, 85 V for 6 h using vertical gel apparatus and visualized by UV shadowing at 254 nm using an AlphaImager (AlphaInnotech, Inc.).

To examine the effect of the FMRP RGG domain binding, a total volume of 15 μL RNA in the presence of desired concentrations of KCl was prepared for each RNA sample, prior to the 5 minutes annealing. Synthetically produced FMRP RGG peptide was added to the RNA in various ratios and incubated for 20 minutes at room temperature. The samples were run on 20% native polyacrylamide gels in 0.5X Tris/Borate/EDTA buffer in the presence of 5 mM KCl at 4°C, 85 V for 6 hours. Electrophoretic motilities of RNA sample were visualized using UV-shadowing at 254nm using an AlphaImager (AlphaInnotech, Inc.).

Fluorescence spectroscopy

Steady-state fluorescence spectroscopy measurements of Shank1a_18AP and Shank1b_24AP RNA binding with the FMRP RGG box, FMRP ISO1 or FMRP S500D were performed on a Horiba Jobin Yvon Fluoromax-3 or on a Horiba Jobin Yvon Fluoromax-4 spectrofluorometer at room temperature. The excitation wavelength was set at 310 nm and the emission spectrum was recorded in the range of 330–450 nm. The bandpass for excitation and emission monochromators were both set to 5 nm. Increasing concentrations of the FMRP RGG peptide or the FMRP isoform was titrated in 50 nM increments to a fixed 200 nM RNA. 1 μM of a peptide derived from the Hepatitis C virus (HCV) core protein or bovine serum albumin (BSA) was added into the RNA sample before titrating RGG peptide and FMRP isoform, respectively. The emission values were corrected and normalized to free RNA fluorescence intensity at 371 nm. Each binding experiment was performed in triplicate. The binding dissociation constant Kd, was determined by fitting the binding curves to the equation:

$$F = 1 + \left(\frac{I_B}{I_F} - 1\right) * \frac{(Kd + [P]t + [RNA]t) - \sqrt{(Kd + [P]t + [RNA]t)^2 - 4 * [P]t * [RNA]t}}{2 * [RNA]t} \quad (4)$$

where I_F and I_B represents the steady-state fluorescence intensities of the free and bound RNA, $[RNA]_t$ is the total concentration of RNA and $[P]_t$ is the total RGG box peptide or FMRP isoform concentration. The reported Kd value is the average from triplicates.

RNA-based affinity pull down assay

Biotinylated HCV RNA control probe (5′ GCC AGC CCC CUG AUG GGG GCG A CACUCC AC CAU GAA U CAC UCC CCU G 3′) was denatured at 95 degrees Celsius for 3 minutes and cooled quickly in a dry ice-ethanol bath. Biotinylated Shank1a and Shank1b RNA probes were denatured at 95 degrees Celsius for 5 minutes and cooled at room temperature for 15 minutes. 5 μM of probe was incubated with E17 mouse brain lysate for 20 minutes at room temperature and NeutrAvidin agarose (Thermo Scientific, Inc.) pre-blocked with BSA was used to precipitate the probes. After extensive washing, proteins were detected by immunoblot against FMRP (1:1250, Sigma) and SMN (1:500, BD Transduction Laboratories).

Disclosure of Potential Conflicts of Interest

No potential conflicts of interest were disclosed.

Funding

This work was supported by the N.I.H. grant 9R15HD078017-03A1 to M.R.M. and R21DA033478 to G.J.B.

References

1. Crawford, DC, Acuña, JM, Sherman, SL. FMR1 and the fragile X syndrome: human genome epidemiology review. Genetics in Medicine 2001, 3(5), 359-371; PMID:11545690; http://dx.doi.org/10.1097/00125817-200109000-00006
2. O ′ Donnell, WT, Warren, ST. A decade of molecular studies of fragile X syndrome. Annual review of neuroscience 2002, 25(1), 315-338; http://dx.doi.org/10.1146/annurev.neuro.25.112701.142909
3. Jin, P, Warren, ST. Understanding the molecular basis of fragile X syndrome. Human molecular genetics 2000, 9(6), 901-908; PMID:10767313; http://dx.doi.org/10.1093/hmg/9.6.901
4. Devys, D, Lutz, Y, Rouyer, N, Bellocq, JP, Mandel, JL. The FMR–1 protein is cytoplasmic, most abundant in neurons and appears normal in carriers of a fragile X premutation. Nature genetics 1993, 4(4), 335-340; PMID:8401578; http://dx.doi.org/10.1038/ng0893-335
5. Bagni, C, Greenough, WT. From mRNP trafficking to spine dysmorphogenesis: the roots of fragile X syndrome. Nature Reviews Neuroscience 2005, 6(5), 376-387; PMID:15861180; http://dx.doi.org/10.1038/nrn1667
6. Ashley, CT, Wilkinson, KD, Reines, D, Warren, ST. FMR1 protein: conserved RNP family domains and selective RNA binding. Science 1993, 262(5133), 563-566; PMID:7692601; http://dx.doi.org/10.1126/science.7692601
7. Siomi, H, Siomi, MC, Nussbaum, RL, Dreyfuss, G. The protein product of the fragile X gene, FMR1, has characteristics of an RNA-binding protein. Cell 1993, 74(2), 291-298; PMID:7688265; http://dx.doi.org/10.1016/0092-8674(93)90420-U
8. Narayanan, U, Nalavadi, V, Nakamoto, M, Pallas, DC, Ceman, S, Bassell, GJ, Warren, ST. FMRP phosphorylation reveals an immediate-early signaling pathway triggered by group I mGluR and mediated by PP2A. The Journal of Neuroscience 2007, 27(52), 14349-14357; PMID:18160642; http://dx.doi.org/10.1523/JNEUROSCI.2969-07.2007
9. Nalavadi, VC, Muddashetty, RS, Gross, C, Bassell, GJ. Dephosphorylation-induced ubiquitination and degradation of FMRP in dendrites: a role in immediate early mGluR-stimulated translation. The Journal of Neuroscience 2012, 32(8), 2582-2587; PMID:22357842; http://dx.doi.org/10.1523/JNEUROSCI.5057-11.2012
10. Santoro, MR, Bray, SM, Warren, ST. Molecular mechanisms of fragile X syndrome: a twenty-year perspective. Annual Review of Pathology: Mechanisms of Disease 2012, 7, 219-245; PMID:22017584; http://dx.doi.org/10.1146/annurev-pathol-011811-132457
11. Penagarikano, O, Mulle, JG, Warren, ST. The pathophysiology of fragile x syndrome. Annu. Rev. Genomics Hum. Genet. 2007, 8, 109-129; PMID:17477822; http://dx.doi.org/10.1146/annurev.genom.8.080706.092249
12. Darnell, JC, Jensen, KB, Jin, P, Brown, V, Warren, ST, Darnell, RB. Fragile X mental retardation protein targets G quartet mRNAs important for neuronal function. Cell 2001, 107(4), 489-499; PMID:11719189; http://dx.doi.org/10.1016/S0092-8674(01)00566-9
13. Menon, L, Mihailescu, MR. Interactions of the G quartet forming semaphorin 3F RNA with the RGG box domain of the fragile X protein family. Nucleic acids research 2007, 35(16), 5379-5392; PMID:17693432; http://dx.doi.org/10.1093/nar/gkm581
14. Hazel, P, Huppert, J, Balasubramanian, S, Neidle, S. Loop-length-dependent folding of G-quadruplexes. Journal of the American Chemical Society 2004, 126 (50), 16405-16415; PMID:15600342; http://dx.doi.org/10.1021/ja045154j
15. Davis, JT. G Quartets 40 Years Later: From 5 ′ GMP to Molecular Biology and Supramolecular Chemistry. Angewandte Chemie International Edition 2004, 43

(6), 668-698; PMID:14755695; http://dx.doi.org/10.1002/anie.200300589
16. Mergny, JL, De Cian, A, Ghelab, A, Sacca, B, Lacroix, L. Kinetics of tetramolecular quadruplexes. Nucleic acids research 2005, 33(1), 81-94; PMID:15642696; http://dx.doi.org/10.1093/nar/gki148
17. Williamson, JR, Raghuraman, MK, Cech, TR. Monovalent cation-induced structure of telomeric DNA: the G-quartet model. Cell 1989, 59(5), 871-880; PMID:2590943; http://dx.doi.org/10.1016/0092-8674(89)90610-7
18. Joachimi, A, Benz, A, Hartig, JS. A comparison of DNA and RNA quadruplex structures and stabilities. Bioorganic & medicinal chemistry 2009, 17(19), 6811-6815; PMID:19736017; http://dx.doi.org/10.1016/j.bmc.2009.08.043
19. Willis, AE. Translational control of growth factor and proto-oncogene expression. The international journal of biochemistry & cell biology 1999, 31(1), 73-86; http://dx.doi.org/10.1016/S1357-2725(98)00133-2
20. Bryan, TM, Baumann, P. G-quadruplexes: from guanine gels to chemotherapeutics. Molecular biotechnology 2011, 49(2), 198-208; PMID:21416200; http://dx.doi.org/10.1007/s12033-011-9395-5
21. Kumari, S, Bugaut, A, Huppert, JL, Balasubramanian, S. An RNA G-quadruplex in the 5′ UTR of the NRAS proto-oncogene modulates translation. Nature chemical biology 2007, 3(4), 218-221; PMID:17322877; http://dx.doi.org/10.1038/nchembio864
22. Subramanian, M, Rage, F, Tabet, R, Flatter, E, Mandel, JL, Moine, H. G–quadruplex RNA structure as a signal for neurite mRNA targeting. EMBO reports 2011, 12(7), 697-704; PMID:21566646; http://dx.doi.org/10.1038/embor.2011.76
23. Drepper, C, Sendtner, M. A new postal code for dendritic mRNA transport in neurons. EMBO reports 2011, 12(7), 614-616; PMID:21681203; http://dx.doi.org/10.1038/embor.2011.119
24. Bassell, GJ, Warren, ST. Fragile X syndrome: loss of local mRNA regulation alters synaptic development and function. Neuron 2008, 60(2), 201-214; PMID:18957214; http://dx.doi.org/10.1016/j.neuron.2008.10.004
25. Darnell, JC, Mostovetsky, O, Darnell, RB. FMRP RNA targets: identification and validation. Genes, Brain and Behavior 2005, 4(6), 341-349; PMID:16098133; http://dx.doi.org/10.1111/j.1601-183X.2005.00144.x
26. Gundelfinger, ED, Boeckers, TM, Baron, MK, Bowie, JU. A role for zinc in postsynaptic density asSAMbly and plasticity. Trends in biochemical sciences 2006, 31(7), 366-373; PMID:16793273; http://dx.doi.org/10.1016/j.tibs.2006.05.007
27. Okabe, S. Molecular anatomy of the postsynaptic density. Molecular and Cellular Neuroscience 2007, 34(4), 503-518; PMID:17321751; http://dx.doi.org/10.1016/j.mcn.2007.01.006
28. Sheng, M, Hoogenraad, CC. The postsynaptic architecture of excitatory synapses: a more quantitative view. Annu. Rev. Biochem. 2007, 76, 823-847; PMID:17243894; http://dx.doi.org/10.1146/annurev.biochem.76.060805.160029
29. Muddashetty, RS, Nalavadi, VC, Gross, C, Yao, X, Xing, L, Laur, O, Warren ST Bassell, GJ. Reversible inhibition of PSD-95 mRNA translation by miR-125a, FMRP phosphorylation, and mGluR signaling. Molecular cell 2011, 42(5), 673-688; PMID:21658607; http://dx.doi.org/10.1016/j.molcel.2011.05.006
30. Boeckers, TM, Bockmann, J, Kreutz, MR, Gundelfinger, ED. ProSAPShank proteins–a family of higher order organizing molecules of the postsynaptic density with an emerging role in human neurological disease. Journal of neurochemistry 2002, 81(5), 903-910; PMID:12065602; http://dx.doi.org/10.1046/j.1471-4159.2002.00931.x
31. Jiang Y Elhers MD. Modelling autism by SHANK gene mutations in mice. Neuron 2013, 78(1), 8-27; PMID:23583105; http://dx.doi.org/10.1016/j.neuron.2013.03.016
32. Böckers, TM, Segger-Junius, M, Iglauer, P, Bockmann, J, Gundelfinger, ED, Kreutz, MR, Richter D, Kindler S, Kreienkamp, HJ. Differential expression and dendritic transcript localization of Shank family members: identification of a dendritic targeting element in the 3′ untranslated region of Shank1 mRNA. Molecular and Cellular Neuroscience 2004, 26(1), 182-190; PMID:15121189; http://dx.doi.org/10.1016/j.mcn.2004.01.009
33. Roussignol, G, Ango, F, Romorini, S, Tu, JC, Sala, C, Worley, PF, Bockaert J Fagni, L. Shank expression is sufficient to induce functional dendritic spine synapses in aspiny neurons. The Journal of neuroscience 2005, 25(14), 3560-3570; PMID:15814786; http://dx.doi.org/10.1523/JNEUROSCI.4354-04.2005
34. Sala, C, Piëch, V, Wilson, NR, Passafaro, M, Liu, G, Sheng, M. Regulation of dendritic spine morphology and synaptic function by Shank and Homer. Neuron 2001, 31(1), 115-130; PMID:11498055; http://dx.doi.org/10.1016/S0896-6273(01)00339-7
35. Schütt, J, Falley, K, Richter, D, Kreienkamp, HJ, Kindler, S. Fragile X mental retardation protein regulates the levels of scaffold proteins and glutamate receptors in postsynaptic densities. Journal of Biological Chemistry 2009, 284(38), 25479-25487; PMID:19640847; http://dx.doi.org/10.1074/jbc.M109.042663
36. Darnell, JC, Van Driesche, SJ, Zhang, C, Hung, KY S, Mele, A, Fraser, CE, Stone EF Darnell, RB. FMRP stalls ribosomal translocation on mRNAs linked to synaptic function and autism. Cell 2011, 146(2), 247-261; PMID:21784246; http://dx.doi.org/10.1016/j.cell.2011.06.013
37. Fürtig, B, Richter, C, Wöhnert, J, Schwalbe, H. NMR spectroscopy of RNA. Chembiochem 2003, 4(10), 936-962; PMID:14523911; http://dx.doi.org/10.1002/cbic.200300700
38. Đapić, V, Abdomerović, V, Marrington, R, Peberdy, J, Rodger, A, Trent, JO, Bates, PJ. Biophysical and biological properties of quadruplex oligodeoxyribonucleotides. Nucleic acids research 2003, 31(8), 2097-2107; PMID:NOT_FOUND; http://dx.doi.org/10.1093/nar/gkg316
39. Williamson, JR. G-quartet structures in telomeric DNA. Annual review of biophysics and biomolecular structure 1994, 23(1), 703-730; PMID:7919797; http://dx.doi.org/10.1146/annurev.bb.23.060194.003415
40. Hardin, CC, Perry, AG, White, K. Thermodynamic and kinetic characterization of the dissociation and assembly of quadruplex nucleic acids. Biopolymers 2000, 56(3), 147-194; PMID:11745110; http://dx.doi.org/10.1002/1097-0282(2000/2001)56:3%3c147::AID-BIP10011%3e3.0.CO;2-N
41. Mergny, JL, Phan, AT, Lacroix, L. Following G-quartet formation by UV-spectroscopy. FEBS letters 1998, 435(1), 74-78; PMID:9755862; http://dx.doi.org/10.1016/S0014-5793(98)01043-6
42. Kelley, SO, Barton, JK. Electron transfer between bases in double helical DNA. Science 1999, 283(5400), 375-381; http://dx.doi.org/10.1126/science.283.5400.375
43. Blice-Baum, A, Mihailescu, R. The Different FMRP Isoforms Bind with High Affinity to the G-Quadruplex formed by the FMRP mRNA. Biophysical Journal 2013, 104, 418; PMID:24249225; http://dx.doi.org/10.1016/j.bpj.2012.11.2331
44. Bole, M, Menon, L, Mihailescu, MR. Fragile X mental retardation protein recognition of G quadruplex structure per se is sufficient for high affinity binding to RNA. Molecular BioSystems 2008, 4(12), 1212-1219; PMID:19396385; http://dx.doi.org/10.1039/b812537f
45. Menon, L, Mader, SA, Mihailescu, MR. Fragile X mental retardation protein interactions with the microtubule associated protein 1B RNA. Rna 2008, 14(8), 1644-1655; PMID:18579868; http://dx.doi.org/10.1261/rna.1100708
46. Zanotti, KJ, Lackey, PE, Evans, GL, Mihailescu, MR. Thermodynamics of the fragile X mental retardation protein RGG box interactions with G quartet forming RNA. Biochemistry 2006, 45(27), 8319-8330; PMID:16819831; http://dx.doi.org/10.1021/bi060209a
47. Antar, LN, Bassell, GJ. Sunrise at the synapse: the FMRP mRNP shaping the synaptic interface. Neuron 2003, 37(4), 555-558; PMID:12597853; http://dx.doi.org/10.1016/S0896-6273(03)00090-4
48. Jin, P, Warren, ST. New insights into fragile X syndrome: from molecules to neurobehaviors. Trends in biochemical sciences 2003, 28(3), 152-158; PMID: AMBIGUOUS; http://dx.doi.org/10.1016/S0968-0004(03)00033-1
49. Veneri, M, Zalfa, F, Bagni, C. FMRP and its target RNAs: fishing for the specificity. Neuroreport 2004, 15(16), 2447-2450; PMID:15538171; http://dx.doi.org/10.1097/00001756-200411150-00002
50. Ceman, S, O′ donnell, WT, Reed, M, Patton, S, Pohl, J, Warren, ST. Phosphorylation influences the translation state of FMRP-associated polyribosomes. Human molecular genetics 2003, 12(24), 3295-3305; PMID:14570712; http://dx.doi.org/10.1093/hmg/ddg350
51. Tarrant, MK, Cole, PA. The chemical biology of protein phosphorylation. Annual review of biochemistry 2008, 78, 797-825; http://dx.doi.org/10.1146/annurev.biochem.78.070907.103047
52. Evans, TL, Blice-Baum, AC, Mihailescu, MR. Analysis of the Fragile X mental retardation protein isoforms 1, 2 and 3 interactions with the G-quadruplex forming semaphorin 3F mRNA. Molecular BioSystems 2012, 8(2), 642-649; PMID:22134704; http://dx.doi.org/10.1039/c1mb05322a
53. Blice-Baum, AC, Mihailescu, MR. Biophysical characterization of G-quadruplex forming FMR1 mRNA and of its interactions with different fragile X mental retardation protein isoforms. RNA 2014, 20(1), 103-114; PMID:24249225; http://dx.doi.org/10.1261/rna.041442.113
54. Li, Y, Tang, W, Zhang, LR, Zhang, CY. FMRP regulates miR196a-mediated repression of HOXB8 via interaction with the AGO2 MID domain. Molecular BioSystems 2014, 10(7), 1757-1764; PMID:24727796; http://dx.doi.org/10.1039/c4mb00066h
55. Edbauer, D, Neilson, JR, Foster, KA, Wang, CF, Seeburg, DP, Batterton, MN, . . . Sheng, M. Regulation of synaptic structure and function by FMRP-associated microRNAs miR-125b and miR-132. Neuron 2010, 65(3), 373-384; PMID:20159450; http://dx.doi.org/10.1016/j.neuron.2010.01.005
56. Laggerbauer, B, Ostareck, D, Keidel, EM, Ostareck-Lederer, A, Fischer, U. Evidence that fragile X mental retardation protein is a negative regulator of translation. Human molecular genetics 2001, 10(4), 329-338; PMID:11157796; http://dx.doi.org/10.1093/hmg/10.4.329
57. Evans, TL, Mihailescu, MR. Recombinant bacterial expression and purification of human fragile X mental retardation protein isoform 1. Protein expression and purification 2010, 74(2), 242-247; PMID:20541608; http://dx.doi.org/10.1016/j.pep.2010.06.002
58. Değerli, N, Akpinar, MA. A novel concentration method for concentrating solutions of protein extracts based on dialysis techniques. Analytical biochemistry 2001, 297(2), 192-194; http://dx.doi.org/10.1006/abio.2001.5335
59. Gasteiger, E, Gattiker, A, Hoogland, C, Ivanyi, I, Appel, RD, Bairoch, A. ExPASy: the proteomics server for in-depth protein knowledge and analysis. Nucleic acids research 2003, 31(13), 3784-3788; PMID:12824418; http://dx.doi.org/10.1093/nar/gkg563
60. Valverde, R, Pozdnyakova, I, Kajander, T, Venkatraman, J, Regan, L. Fragile X mental retardation syndrome: structure of the KH1-KH2 domains of fragile X mental retardation protein. Structure 2007, 15(9), 1090-1098; PMID:17850748; http://dx.doi.org/10.1016/j.str.2007.06.022
61. Piotto, M, Saudek, V, Sklenář, V. Gradient-tailored excitation for single-quantum NMR spectroscopy of aqueous solutions. Journal of biomolecular NMR 1992, 2(6), 661-665; PMID:1490109; http://dx.doi.org/10.1007/BF02192855